Welding Process Effects in Weldability Testing of Steels

Minimum preheats for avoiding weld deposit hydrogen-induced cracking can depend on the welding process used

BY G. ATKINS, D. THIESSEN, N. NISSLEY, AND Y. ADONYI

ABSTRACT. This work was part of a nationwide program for the development of new high-performance steels with 70 ksi (485 MPa) minimum yield strength, improved toughness, and lower manufacturing costs through the elimination of preheat for welding. The purpose of the present work was to evaluate the fusion zone hydrogen-induced cracking susceptibility of single-pass weld deposits made using four different welding processes at equivalent diffusible hydrogen levels. The gapped bead-on-plate test was used to compare shielded metal arc (SMAW), submerged arc (SAW), gas metal arc (GMAW), and flux cored arc (FCAW) welding processes. Equivalent net heat inputs were produced and the weld cross-sectional areas were normalized at different arc energies, including the heat transfer efficiency for each process.

The minimum predicted preheats were different, lower for SAW than for GMAW, FCAW, and SMAW at similar diffusible hydrogen levels and heat inputs. This difference was attributed to the different solidification microstructures and weld bead geometries. Preheating guidelines based on the SMAW process remained the most conservative, confirming the validity of the past practice of using SMAW to find minimum preheats. It was concluded that preheat recommendations should not be extrapolated from one welding process to another. The information generated was used for manufacturing recommendations for welding high-performance steels.

Background

Future construction and retrofitting of bridges involves the search for economical and safe methods of manufacturing. Weathering steels such as USS Cor-Ten (ASTMA 485W) have traditionally offered significant cost savings to the bridge industry due to their ability to resist corrosion without paint. Corrosion damage and prevention can be a significant factor in bridge maintenance costs, reaching up to 30% of initial costs. Improvements in steel manufacturing processes such as vacuum degassing, lowering carbon and sulfur content, and the addition of calcium for sulfide shape control resulted in high-performance steels (HPS). These steels have good corrosion resistance, up to 100 ksi (690 MPa) yield strength, low yield-to-tensile strength ratio, and high toughness (Refs. 1, 2).

Modern high-performance weathering steels offer many advantages to the bridge industry, such as high strength, excellent toughness, and less variability in properties between heats of steels. In order for these high-performance steels to be considered by the bridge construction industry, realistic welding procedures must be developed that will capitalize on the cost saving aspects of the steels. One such target was reduction or elimination of preheat to lower fabrication costs. Indeed, with the lower hardenability in the heat-affected zone (HAZ), preheat might not be needed to avoid hydrogen-induced cracking. However, the weld deposit is usually an as-cast microstructure where only chemistry and solidification morphology can be used to control cold cracking susceptibility. Therefore, cracking susceptibility in these high-strength steels can be expected to be higher in the weld fusion zone (FZ) rather than in the HAZ (Refs. 1, 2).

KEY WORDS

Weldability Testing
SAW, GMAW,
FCAW, SMAW
Gapped Bead-on-Plate (G-BOP)
G-BOP Testing
High-Performance Steels
Weathering Steels
Hydrogen-Induced Crack

Introduction

Hydrogen-induced cracking of weld deposits for joining HPS (A 485W or HPS 70W) quenched-and-tempered steel, 2-in.- (50.8-mm-) thick plate has been extensively evaluated using the gapped bead-on-plate (G-BOP) test (Refs. 3, 4) — Figs. 1, 2. This test was chosen from many simulative weldability tests for two reasons: simplicity and reliability in quantifying weld fusion zone cracking susceptibility as opposed to HAZ cracking (Refs. 5, 6). Initially, most tests used the submerged arc welding (SAW) process because bridge fabricators were the first users of this weathering 70 ksi HPS, or HPS 70W.

The HAZ of HPS 70W has particularly low hardenability (P_{cm} = 0.256) because of low carbon content, small HAZ grain size, and bainitic microstructure that reaches only 300–350 HV maximum. Previous Tekken (Y-groove) testing showed these steels do not need preheat to avoid hydrogen-induced cracking in the HAZ for thicknesses up to 2 in. and low (up to 4 mL/100g) diffusible hydrogen (Ref. 3).

Therefore, minimum preheat levels for the weld fusion zone had been established for different electrode wire/flux combinations, heat inputs, and electrode polarity using the G-BOP test. However, when trying to compare results with those obtained by previous investigators who used the shielded metal arc welding (SMAW) process, it became obvious that for all conditions being equal, use of the SMAW process predicted higher minimum preheat temperatures than the SAW process (Refs. 7–9).

It was hypothesized there were several reasons for this difference. First, the weld

G. ATKINS is Research Associate, D. THIESSEN, former Research Associate, is currently with CB&I, and N. NISSLEY, former Research Associate, is currently a graduate student at The Ohio State University, Columbus, Ohio. Y. ADONYI is Professor and Omer Blodgett Chair of Welding and Materials Joining Engineering at LeTourneau University, Longview, Tex.

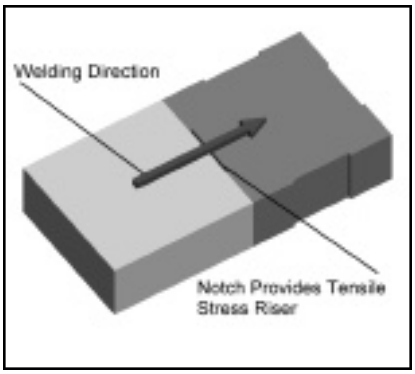

Fig. 1— Schematic representation of the gapped bead-on-plate (G-BOP) test showing the machined notches and welding direction.

deposit strength was different between the two processes, as confirmed by microstructural evaluation and hardness measurements. Indeed, the SMAW average hardnesses were consistently 30–40 HV higher than the SAW hardnesses for similar net heat inputs. The relative volume fraction of martensite was also higher and the crack surfaces exhibited mostly cleavage features (Refs. 7, 8). Secondly, variability in weld fusion zone microstructure due to segregations during solidification added to variability in results because of the mixed (brittle/ductile) failure modes often encountered in G-BOP tests — Fig. 3. Additionally, the weld deposit geometries were different because of the typically smaller penetration inherent to the SMAW process (35–45% dilution) as compared to the SAW process (55–65% dilution, Ref. 3). These lower depth-to-width ratios in SMAW were predicted to result in a higher stress concentration at the weld root during cooling of the G-BOP specimens (see result of FEA prediction, Fig. 4, Ref. 10).

At the same time, no data was available on preheat temperatures when using gas-shielded arc welding processes such as the gas metal arc (GMAW) and flux cored arc (FCAW) welding processes. Traditional lack of acceptance of gas-shielded arc welding processes by the bridge industry was the reason for not looking at these processes originally. However, as new welding wires (solid and metal cored) with matching strength, weathering resistance, and good toughness became available, the need arose to compare the cracking susceptibility of these processes in welding HPS steels.

Objective

The scope of this work was to determine the effect of welding processes on hydrogen-induced cracking susceptibility of HPS 70W weld deposits. Minimum preheats predicted by using the G-BOP test were compared when using the SAW, SMAW, FCAW, and GMAW processes at various diffusible hydrogen levels.

Table 1 — Average Chemical Composition of the HP 70W and A 485W Steels (wt-%)

	C	Mn	Si	P	S	Cu	Ni	Cr	Al	Ce_{IIW}
HP70W	0.10	1.20	0.30	0.006	0.003	0.45	0.35	0.52	0.030	0.319
A 485W (Cor-Ten)	0.20	0.90	0.40	0.010	0.020	0.30	0.30	0.40	0.025	0.410

Other elements: 0.00094% B, 0.001% Sb, 0.006% As

Table 2 — Typical Room Temperature Mechanical Properties of HP 70W Steel As Compared with the Traditional Cor-Ten

Steel Type	Ultimate Tensile Strength (ksi)	Yield Strength (ksi)	Yield/ Tensile Ratio	Elongation %	Impact Toughness CVN @ –10F (ft-lb)
HP 70W	94	80	0.85	71	172–264
ASTM A 485W	90	85	0.94	65	120–150

Table 3 — Manufacturer's Reported Typical Weld Metal Deposit Chemistry

Welding Process	C	Mn	Si	P	S	Cr	Ni	Cu	V	Mo
FCAW E71T-1 (Ref. 14)	0.05	1.16	0.31	0.008	0.012	—	—	—	—	—
SMAW E9018-G (Ref. 15)	0.05 — 0.09	1.30 — 1.60	0.30 — 0.60	0.025 max	0.020 max	0.08 max	0.60 — 0.95	—	0.015 max	0.05 max
GMAW ER80S-G (Ref. 16)	0.10	0.551	0.23	0.014	0.009	0.45	0.55	0.45	—	—
SAW F7A6-EH12K-H8 (Ref. 17)	0.09	1.43	0.38	0.014	0.004	—	—	0.10	—	—

Methodology

Base Metal and Welding Consumables Used

A preliminary parametric study was performed on bead-on-plate weld deposits using the four welding processes to be evaluated. The objective was to find arc energies that would produce equivalent net heat inputs and weld deposit geometries to accurately compare G-BOP cracking results. The base metal used was 2-in.- (50.8-mm-) thick HPS 70W plate for all experiments. The chemical composition and mechanical properties of the high-performance steel are shown in Tables 1 and 2. Note the steel has a leaner composition than its traditional ASTM A 485W counterpart (Cor-Ten), reflected in the lower hardenability or carbon equivalent (C_e) number. Also note the low sulfur content, which, together with the morphology of the evenly distributed spherical sulfides, accounts for the excellent toughness of this steel.

The procedure of performing gapped bead-on-plate testing has been described elsewhere (Ref. 3). In essence, two blocks of 2-in.- (50.8-mm-) thick steel are clamped together in a device, with a small gap (approximately 0.020 to 0.050 in.) machined in one of the blocks. As the finite element analysis (FEA) model in Fig. 4 shows, high stresses develop at the root of the weld after the bead is deposited over this gap. Welding this deposit in the presence of diffusible hydrogen can cause delayed root cracking in the weld fusion zone. The purpose of the test is to find a minimum preheat temperature at which cracking can be eliminated.

In this work, a modern inverter-based power supply and a digital-controlled

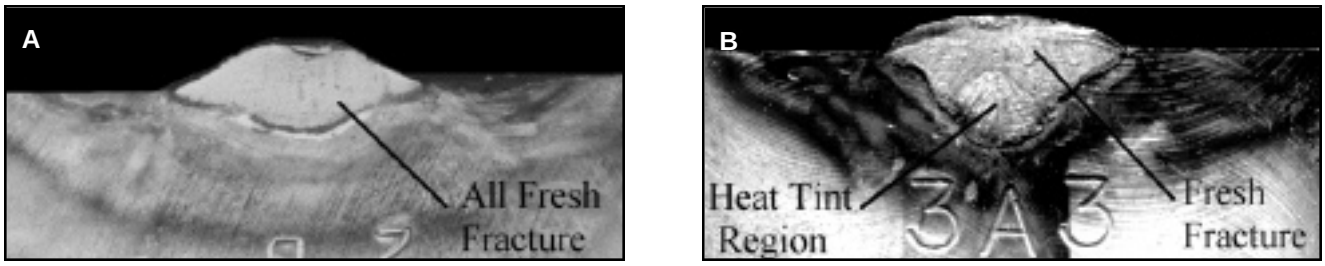

Fig. 2 — Gapped bead-on-plate test evaluation criteria, view of weld beads broken cross section following heat tinting to mark the hydrogen-induced crack. A — 0% cracking; B — 30% cracking.

wire feeder were used to improve the accuracy and repeatability of testing. A constant-current power supply was used for the SMAW. A motorized carriage with digital speed readout was used to control the travel speed for all torch movements (the SMAW was guided with its help).

The welding consumables used provided for a "matching" deposit (i.e., for 70 ksi, 485 MPa, minimum yield strength). Shielded metal arc (E9018-M) electrodes were partially baked at the manufacturer to provide H4, H8, and H16 (4, 8, and 16 mL/100g) diffusible hydrogen levels, respectively. Figure 5A shows the experimental setup used to weld diffusible hydrogen samples, while Fig. 5B shows the mechanized setup for SMAW maintaining constant weld travel speed during G-BOP testing. The GMA welding wire was a 0.045-in.- (1.14-mm-) diameter ER80S-G solid wire. For FCAW, a E71T-1 tubular wire was used. A standard 75% Ar-25% CO_2 gas mixture was used for the reference experiments. The typical all-weld-metal chemical compositions and mechanical properties are shown in Tables 3 and 4. Also, the G-BOP weld bead hardness for each process is shown in Table 5.

Diffusible Hydrogen

For GMAW and FCAW processes, hydrogen was added to the shielding gas through a precision flow meter — Fig. 6. Two bottles of gas were used, one with the standard 75% Ar-25% CO_2 mixture, the other special 72.5 % Ar-22.5% CO_2-5% H_2. The relationship between the amount of hydrogen mixed in the GMAW shielding gas and the diffusible hydrogen measured in the weld deposit increased as shown in Fig. 7 (also Tables 7 and 9). Note the nonlinear nature of the relationship in Table 8. This is most likely caused by the kinetics of dissociation and recombination of the atomic hydrogen. Excess hydrogen did not increase the diffusible (atomic) hydrogen content in the weld but resulted in entrapped gas pockets and wormholes in the deposit — Fig. 8.

Table 4 — Manufacturer's Reported Typical Weld Metal Mechanical

Welding Process	Tensile Strength ksi (MPa)	Yield Strength ksi (MPa)	Elongation (%)	Charpy V-notch ft-lb (J)
FCAW				101 (137) @ 0°F (–18°C)
E71T-1	84 (597)	77 (531)	28	90 (122) @ –40°F (–40°C)
(Ref. 14)				53 (72) @ –60°F (–51°C)
SMAW				77 (104) @ –20°F (–29°C)
E9018-G	99 (683)	89.9 (530)	29	53 (72) @ –50°F (–46°C)
(Ref. 15)				
GMAW				
ER80S-G	78.5 (542)	72.5 (500)	24	25 (34) @ –20°F (–29°C)
(Ref. 16)				
SAW				
F7A6-EH12K-H8	80.7 (556)	87.2 (601)	30	122 (152) @ –60°F (–51°C)
(Ref. 17)				

Table 5 — Vickers Hardness Values of G-BOP Fusion Zones

Welding Process	20 kJ/in. Heat Input HV	40 kJ/in. Heat Input HV
FCAW	N/A	217
SMAW	273	278
GMAW	251	227
SAW	273	280

Table 6 — Correlation Between the Hydrogen Added to the Shielding Gas and the Actual Diffusible Hydrogen Entrapped in the Weld

Hydrogen in Gas Mixture Hydrogen %	Diffusible mL/100 g
0.5	6.4
1.0	8.7
2.0	12.4
4.0	16.5

For flux-assisted welding processes (SMAW and SAW), target diffusible hydrogen levels were obtained by partial baking of the coating at the manufacturer (SMAW) and flux humidification in the lab (SAW) (Ref. 3). Due to difficulty in controlling the exact amounts, certain ranges were obtained, categorized as low (below 5 mL/100g), medium (5–10 mL/100g), and high (above 10 mL/100g). Figure 9 shows the effect of diffusible hydrogen on cracking for the SAW, SMAW, and GMAW welding processes.

All diffusible hydrogen was tested according to ANSI/AWS A 4.3, Standard Methods for Determination of the Diffusible Hydrogen Content of Martensitic, Bainitic, and Ferritic Steel Weld Metal Produced by Arc Welding. The collection of diffusible hydrogen specimens was performed immediately prior to G-BOP testing (i.e., at the same environmental conditions, using the same welding setup and consumables).

Results and Discussion

Heat Input Equivalency Determination

In order to compare these four welding processes, the heat transfer efficiencies had to be examined. It had been long known that different welding processes have different heat and melting efficiencies (Refs. 11, 12). The net heat input in any arc welding process can be written as

$$Q_{net} = h \times Q_{arc} \quad [cal] \qquad (1)$$

where Q_{net} = net heat input; Q_{arc} = arc

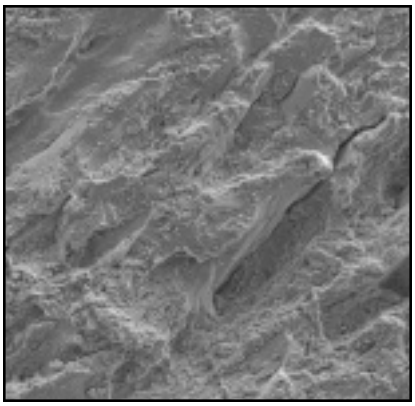

Fig. 3 — Typical scanning electron microscopy fractographs showing the mixed mode of cracking in G-BOP weld deposits (brittle cleavage and ductile dimples), 1000X magnification.

Table 7 — The Effect of Hydrogen Added to the Gas As Well As the Resulting Diffusible Hydrogen on G-BOP Cracking

Process/ Wire	% Hydrogen Added	Diff. Hydrogen mL/100 g	Cracking %
	Base Line	3.5	1
FCAW/	2	12.4	77
E71T-1	4	16.5	100
	Base Line (baked)	1.7	5
GMAW/	0.5	6.4	50
ER80S-G	1	8.7	83

Table 8 — Calculated Heat Transfer Efficiencies Based on Weld Cross-Sectional Areas

Process	Welding Current A	Arc Voltage V	Travel Speed in./min	Arc Energy kJ/in.	Theoretical Heat Input kJ/in.	Heat Transfer Efficiency η
FCAW	189	26	12	24	20	0.83
	238	28	9.2	43.4	40	0.92
GMAW	171	27	12	23	20	0.86
	250	28	9.2	46	40	0.87
SMAW	180	24	10.9	23.5	20	0.85
	220	24	7.1	44.6	40	0.89

Table 9 — Theoretical Variation of Weld Deposit Yield Strength with Heat Input for Three Welding Processes

Welding Process	Theoretical Heat Input kJ/in.	Theoretical Cooling Rate F/s	Theoretical Yield Strength ksi
GMAW-S	20	116	91
	40	70	96
SMAW	20	100	102
	40	60	94
SAW	20	83	96
	40	40	86

Table 10 — SAW Results, G-BOP Tests (Ref. 3)

Wire/Flux	Arc Energy kJ/in.	Diff. Hydrogen mL/100 g	Preheat F	% Cracking
F7A6-EH12K-H8	40	1.8	50	0
			72	0
			125	0
			225	0
F7A6-EH12K-H8	40	5	50	3
			72	0
			125	0
			225	0
F7A6-EH12K-H8	40	7.4	50	80
			72	50
			125	0
			225	0

Based on previous work (Ref. 3), the G-BOP results in Tables 10 and 11 were chosen for comparison.

energy, kJ/in.; and η = heat transfer efficiency (a product of the arc efficiency, η_{arc} times the melting efficiency, η_{melt}), always less than 1.0

$$Q_{arc} = (E \times I)/s \times 60 \qquad [J/in.] \quad (2)$$

where E = arc voltage, volts; I = welding current, amperes; and s = travel speed, in./min.

Each arc welding process has been found to have different energy losses through the arc via radiation, convection, etc. Therefore, each welding process will yield a different heat transfer efficiency range. They are as follows:

SAW, η = 0.9–0.95,
GMAW, η = 0.7–0.85,
FCAW, η = 0.7–0.8,
SMAW, η = 0.65–0.7 (Ref. 10).

Because of η ~ close to 1.0 for SAW, the arc energy is $Q_{arc} \sim Q_{net}$. For the other welding processes, however, this extrapolation from Q_{arc} to Q_{net} cannot be made. Thus, comparing welding processes with equal arc energies result in erroneous heat inputs of up to 35% lower than expected (see SMAW η = 0.65–0.7).

The net heat input (Q_{net}) can be quantified experimentally. Knowing that

$$Q_{net} = Q_{melt} + Q_{cond} + Q_{rad} + Q_{conv} \quad (3)$$

one can assume that for a given material, setup, thickness, etc., the conductive, convective and radiative heat components are equal. Therefore, the only difference remains in melting a given mass of metal. Assuming equal metal density, the volume of the deposit will be proportional with the net heat input (Ref. 11). For the same weld length, the cross-sectional area is a good indicator of the net heat input. Therefore, any true comparative study between processes has to "normalize" the weld cross sections.

Because the above four welding processes have different heat transfer efficiencies, measuring HAZ cooling rates and comparing them to the weld cross-sectional area has been shown to be effective in finding the arc energies that produce equivalent heat inputs.

Weld Cross-Sectional Area Normalization for Heat-Input Equivalency Determination

Two net heat inputs were targeted based on previous SAW results: 20 and 40 kJ/in., respectively. The corresponding cross-sectional areas of the weld beads were 0.04 ± 0.005 $in.^2$ (0.26 ± 0.03 cm^2) for 20 kJ/in. (0.8 kJ/mm) and 0.07 ± 0.005 $in.^2$ (0.45 ± 0.03 cm^2) for 40 kJ/in. (1.6 kJ/mm).

The only purpose of this set of experiments was to obtain equivalent net heat inputs and similar cooling rates. Without

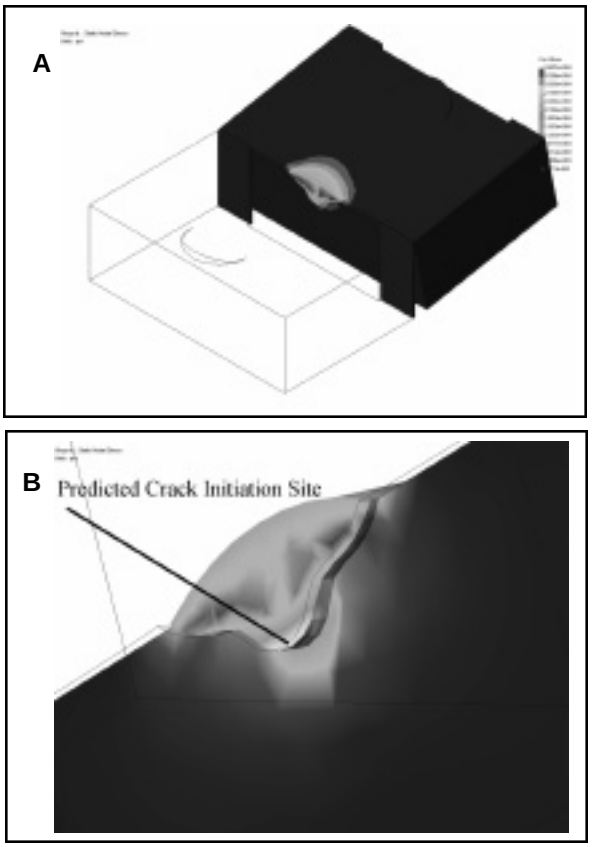

Fig. 4 —Finite element modeling results showing stress buildup at the root of the G-BOP test block where cracking typically initiates. A — Top view; B — cross-section view; C — bottom view.

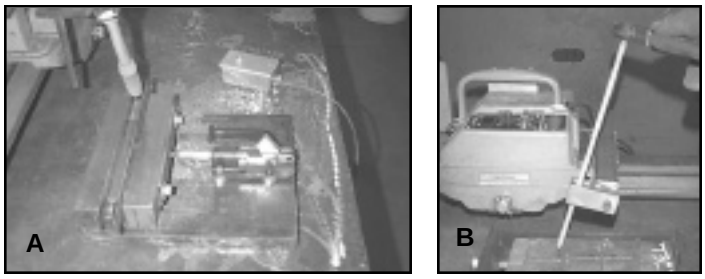

Fig. 5 — A — View of the diffusible hydrogen measurement; B — mechanized SMAW experimental setup used for G-BOP welding.

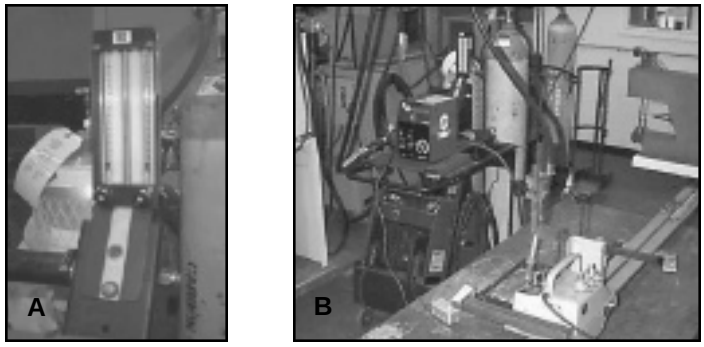

Fig. 6 — A — View of the experimental setup used for mixing hydrogen into the shielding gas; B — GMAW/FCAW welding of the G-BOP test.

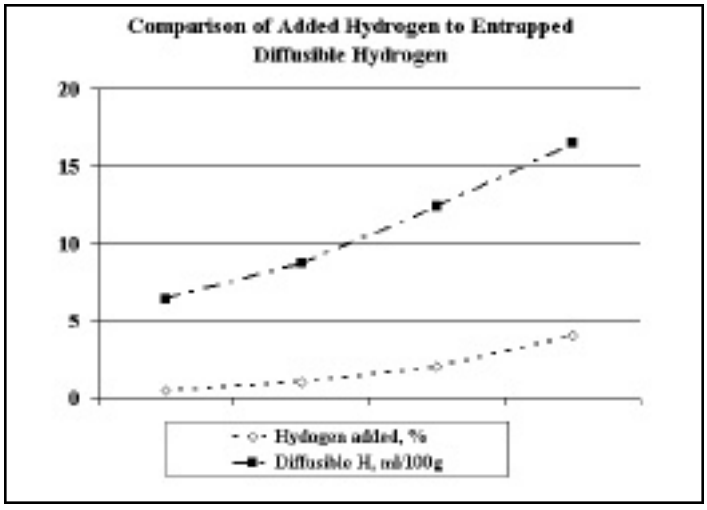

Fig. 7 — Correlation of the percent hydrogen volume added to the shielding gas and diffusible hydrogen entrapped in the weld bead.

this normalization, the cooling rates and resulting weld deposit properties could be so different that comparison of hydrogen-induced cracking data might be very difficult.

The predictive software (Ref. 13) used by the Navy Surface Warfare Research Center (NSWRC) incorporated these different heat transfer efficiencies. The results are shown in Table 9. Table 8 shows the results of using digital image analysis of typical SAW, SMAW, GMAW, and FCAW weld cross-section photomacrographs. There was scatter in dilution results, although most values were around 50% for SMAW and 60% for SAW.

Previous calculations (Ref. 3) have also shown a 20% difference can be expected between the heat transfer efficiencies of the SMAW vs. the SAW welds. Indeed, comparing the 20 kJ/in. (0.8 kJ/mm) arc energy SAW and 25 kJ/in. (1.0 kJ/mm) arc energy SMAW, there was a fairly good correlation between the measured weld areas and corresponding weld hardnesses. The SMAW weld deposit hardnesses were on the average 30–40 HV higher than the corresponding SAW welds. This variation in weld deposit hardness with welding process was confirmed using an analytical model (Ref. 13). Table 7 shows that for equivalent arc energies, the theoretical yield strengths were different for SAW, SMAW, and GMAW weld deposits. All calcula-

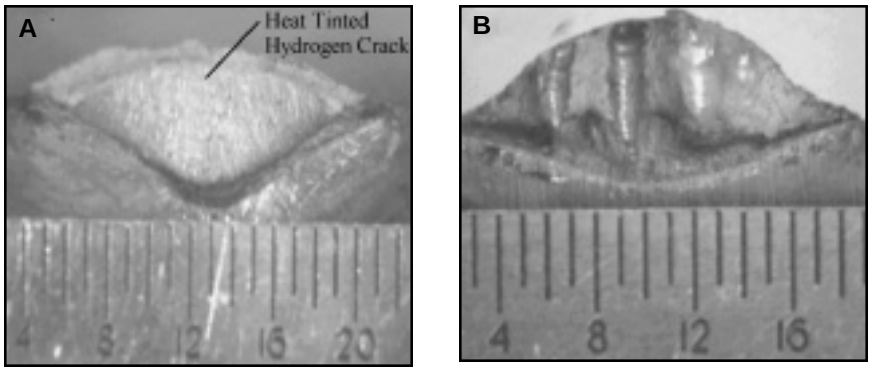

Fig. 8 — Typical extensive cracking when using SMAW process (a) and wormholes resulting from molecular hydrogen trying to escape from the pool (b).

Table 11 — SMAW G-BOP Results (Ref. 3)

Electrode	Arc Energy kJ/in.	Diff. Hydrogen mL/100 g	Preheat F	% Cracking
E9018-M	40	4.0	72	100
			125	90
			225	0
			275	0

Table 12 — GMAW Results G-BOP, Current Work

Electrode	Arc Energy kJ/in.	Diff. Hydrogen mL/100 g	Preheat F	% Cracking
ER80S-G	40	1.7	70	5
			125	1
			225	0
			275	0
ER80S-G	40	6.4	70	58
			125	5
			225	1
			275	0
ER80S-G	40	8.7	70	90
			125	60
			225	33
			275	0

Table 13 — FCAW G-BOP Results

Electrode	Arc Energy kJ/in.	Diff. Hydrogen mL/100 g	Preheat F	% Cracking
E71T-1	40	12.4	72	51
			125	15
			225	0
			275	0

tions were made assuming single-pass, bead-on-plate welds. These predictions underline the basic differences between the welding processes compared in this study. For the same net heat input of 20 kJ/in. (0.8 kJ/mm), for example, cooling rate variations from 40 to 70°F/s (22 to 39°C/s from SAW to GMAW), and deposit strength variations of more than 10% from 86 to 96 ksi (593–662 MPa) can be expected. However, these differences become smaller at higher arc energy.

For the final G-BOP testing and evaluation, a heat input value of 40 kJ/in. (1.6 kJ/mm) was chosen to compare the four welding processes (SAW, GMAW, FCAW, and SMAW) for the following reasons:

- Extensive cracking was experienced at the lower end of 20 kJ/in., making a comparison between the four processes very difficult.
- Cooling rate and deposit strength variation decrease as heat input is increased.
- All four welding processes easily produce a good weld with reproducible shape and cross section at 40 kJ/in.

Relative G-BOP Cracking Susceptibility: SAW, SMAW, GMAW, and FCAW

Cracking susceptibility of the four welding processes was evaluated based on a net heat input of 40 kJ/in. (1.6 kJ/mm). The minimum preheat to prevent cracking for each welding process (except GMAW, which is known to be a low-hydrogen process) was based on the worst-case scenario (i.e., highest diffusible hydrogen) for each welding process in the G-BOP tests.

SAW Process, G-BOP Results

Based on previous work (Ref. 3), the G-BOP results shown in Table 10 were chosen for comparison. When comparing these results to those shown in Table 11 for the SMAW process, as well as the data included in Ref. 3, the preheat levels needed to avoid cracking were, in general, lower in the SAW than the SMAW process. A minimum preheat of 125°F (52°C) would be sufficient for SAW to avoid cold cracking in all conditions investigated. Figure 10 shows the SAW fusion zone microstructure, which is a mostly fine pearlitic structure with signs of columnar growth.

SMAW Process, G-BOP Results

For this part of the experiments, an E9018 electrode was used. The results are shown in Table 9, as compared with previous results. It became clear that for

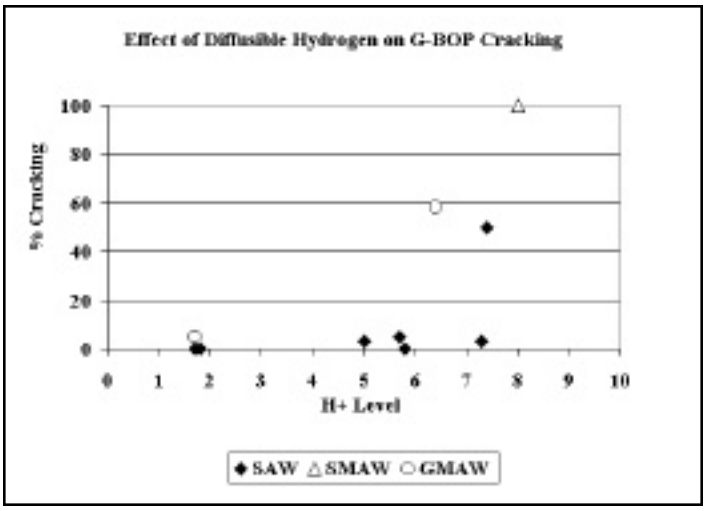

Fig. 9 — Effect of diffusible hydrogen on G-BOP cracking at room temperature for the three welding processes used.

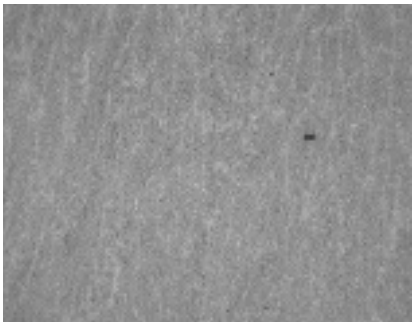

Fig. 10 — SAW G-BOP fusion zone microstructure, 2% Nital etch, 100X.

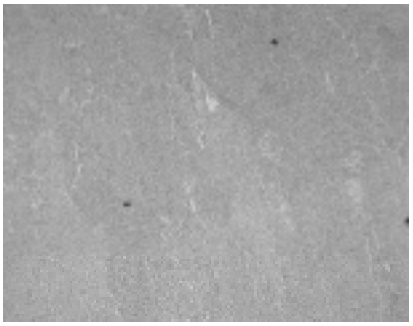

Fig. 11 — SMAW G-BOP fusion zone microstructure, 2% Nital etch, 100X.

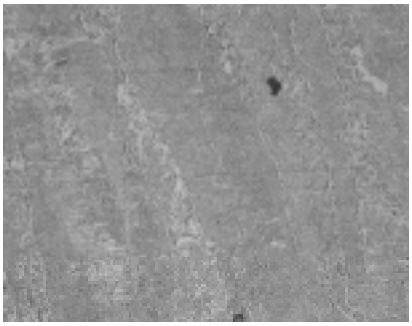

Fig. 12 — GMAW G-BOP fusion zone microstructure, 2% Nital etch, 100X.

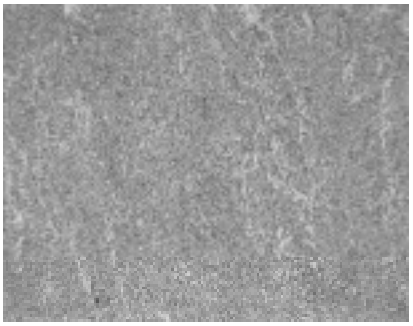

Fig. 13 — FCAW G-BOP fusion zone microstructure, 2% Nital etch, 100X.

these diffusible hydrogen levels, only a minimum preheat of 225°F (107°C) (100°F, or 56°C, higher than for the SAW process) would be sufficient to avoid cold cracking for the conditions tested. The SMAW fusion zone microstructure is shown in Fig. 11. The evidence of columnar solidification can also be seen in Fig. 11. The majority of the matrix is pearlite with pockets of ferrite.

GMAW Process, G-BOP Results

For this part of the experiments, a matching consumable and three diffusible hydrogen levels were chosen. The results are shown in Table 12. For the conditions investigated, or low-to-high diffusible hydrogen, only a minimum preheat of 275°F (135°C) would avoid cold cracking. Realistically, however, GMAW is known to be a low-hydrogen process, therefore, the results from 1.7 mL/100 g diffusible hydrogen could be used (minimum preheat of 125°F or 52°C). The fusion zone microstructure can be seen in Fig. 12. The columnar growth of the GMAW fusion zone is much more apparent than that seen in the submerged arc or shielded metal arc welds. While the structure is mostly dominated by pearlite, the presence of pure ferrite is strong at the columnar boundaries.

FCAW Process, G-BOP Results

For this part of the experiments, a matching wire was used at two diffusible hydrogen levels (Table 13). For the conditions investigated (low-to-high diffusible hydrogen), a minimum preheat of 225°F (107°C) would be needed to avoid cold cracking. Because FCAW can be a rather high diffusible hydrogen process, this particular preheat would be more conservative. Figure 13 shows a typical FCAW fusion zone microstructure, which is a fine pearlite matrix.

Comparing the results between the G-BOP cracking data (Fig. 14), the SAW welding process showed the least susceptibility to hydrogen-induced cracking, while SMAW and FCAW resulted in high preheat predictions. While variability in weld deposit geometry, microstructure, hardness, and diffusible hydrogen levels used in this comparison could be affecting the results, the trends indicate extrapolating the results from one welding process to another might not be adequate. Therefore, it is believed simulative testing traditionally performed using the worst case scenario (SMAW, low heat input levels) remains an acceptable practice. However, when other low-hydrogen welding processes are to be used, lower or no preheat conditions might be expected, depending on base metal type, thickness, and joint geometry.

Conclusions

1) The bead-on-plate parameter optimization resulted in similar weld cross-sectional areas, but different dilutions for the four welding processes compared.

2) G-BOP testing resulted in the following ranking among welding processes (from least to most susceptible) for equivalent net heat inputs, weld deposit nominal strength, and diffusible hydrogen levels (Table 14):

- SAW (125°F min. preheat)
- GMAW (125°F min. preheat)
- FCAW (225°F min. preheat)
- SMAW (225°F min. preheat)

3) Extrapolating weldability test results from one welding process to another

Table 14 — Worst-Case Scenario Comparative G-BOP Results, FCAW vs. SMAW vs. GMAW vs. SAW

Process	Heat Input kJ/in.	Diff. Hydrogen mL/100 g	Preheat F	% Cracking
FCAW	40	12.4	70	51
			125	15
			225	0
			275	0
SMAW	40	4.0	72	100
			125	90
			225	0
			275	0
GMAW	40	8.7	70	90
			125	60
			225	33
			275	0
SAW	40	7.4	50	80
			72	50
			125	0
			225	0

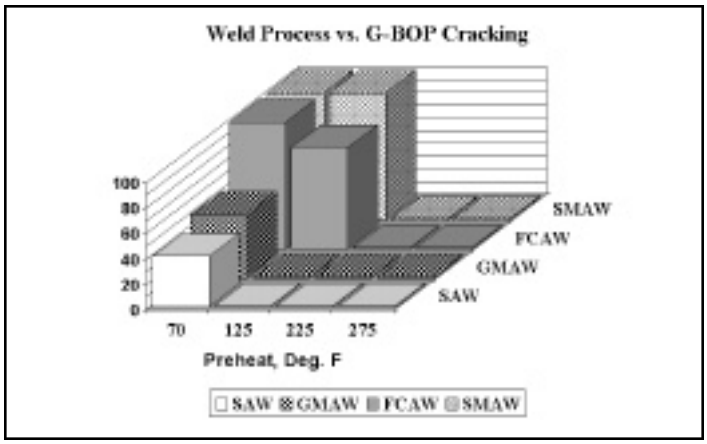

Fig. 14 — Comparative results of G-BOP cracking for equivalent heat inputs and 5–7 mL/100 g diffusible hydrogen.

is not recommended, except for the widely accepted practice of using SMAW as the most conservative predictor of preheat temperatures.

Acknowledgments

The authors would like to thank the Federal Highway Administration Research Lab, American Iron and Steel Institute, and the United States Navy Surface Warfare Center, Carderock Division for funding the work and providing guidance. Also, we would like to thank The Lincoln Electric Co. and ESAB for providing the welding consumables. The contribution of the following LeTourneau University students is also acknowledged: H. Vogel, T. Olson, D. Mast, and M. Coker.

References

1. Fisher, J. W., Dexter, R. J. 1994. High-performance steels for America's bridges. Welding Journal 73(1): 35–43.

2. Wilson, A. 1999. High performance weathering steel properties. Proceedings of the International Conference on High Performance Steels. Cincinnati, Ohio.

3. Adonyi, Y. 1998. Weldability Testing of the High-Performance 70 ksi Weathering Steel. Report prepared for NSWC/FHWA, LeTourneau University. Available through the American Iron and Steel Institute (AISI).

4. Adonyi, Y. 1998. Submerged arc weld deposit property evaluation for high-performance 100 W steels. Unpublished report, LeTourneau University.

5. Graville, B. A. 1994. Interpretive report on weldability tests for hydrogen cracking of higher strength steels and potential for standardization. Prepared for the Welding Research Council.

6. Chakravarti, A. P., Bala, S. R. 1989. Evaluation of weld metal cold cracking using the G-BOP test. Welding Journal 68(1): 1-s to 8-s.

7. Masubuchi, K. 1980. Analysis of Welded Structures, New York, N.Y: Pergamon Press.

8. Yurioka, et al. 1988. Heat-affected zone hardness of SAW weld metals. IIW-Document IX-1524-88.

9. Yurioka, N. 1990. Weldability of modern high-strength steels. First United States-Japan Symposium on Advances In Welding Metallurgy, pp. 51–64. Miami Fla.: American Welding Society.

10. Nissley, N. 1999. Weld geometry effects in weldability testing of high-performance steels. paper presented at the 79th Annual AWS Show and Conference, St. Louis, Mo.

11. DuPont, J. N., Marder, A. R., 1995. Thermal efficiency of arc welding processes. Welding Journal 74(12): 406-s to 416-s.

12. Niles, R., Jackson, C. E. 1975. Welding thermal efficiency of the GTAW process. Welding Journal 54(1): 25-s to 32-s

13. Wong, R. 1999. United States Navy Surface Warfare Research Center, Carderock Division. Private communications.

14. ESAB catalog. Retrieved 2001, from http://www.esab.com

15. The Lincoln Electric. Co. Retrieved 2001, from http://lincolnelectric.com

16. ESAB catalog. Retrieved 2001, from http://www.esab.com

17. Teresa Melfi. The Lincoln Electric Co., Cleveland, Ohio. 2001. E-mail communication.